

Simulation of 3D Block Populations to Characterize Outcrop Sampling Bias in Bimrocks

By William C. Haneberg

Block-in-matrix rocks (bimrocks) are defined as “a mixture of rocks, composed of geotechnically significant blocks within a bonded matrix of finer texture” (1), a definition that encompasses a wide range of geologic materials including melanges, fault rocks, landslide debris, and glacial till.

Figure 1 shows a typical bimrock, in this case an outcrop of Mesozoic Franciscan Complex melange near Mendocino, California, USA. In this example the blocks visible in the outcrop are on the order of centimeters to decimeters in their longest dimension, but in other places they can range in size from meters to hundreds of meters in length. The geotechnical significance of bimrock blocks was illustrated by Lindquist (2) and Lindquist and Goodman (3), who showed that in physical models of melange, the angle of internal



Fig. 1 Typical bimrock outcrop of Franciscan Complex melange near Mendocino, California, USA. The white disk near the center of the photograph is a 2.3 cm diameter coin. (Photo courtesy of Ed Medley, 1994).

Bild 1 Typischer „Bimrock“-Aufschluss in San Franciscan Melange in der Nähe von Mendocino, Kalifornien, USA. Die weiße Scheibe in Fotomitte stellt eine Münze mit 2,3 cm Durchmesser dar (Foto Ed Medley, 1994).

friction increased and the cohesive strength decreased as a function of block proportion in cases where block proportions exceeded 25 to 30 %.

The standard engineering practice is to use the strength of the weakest component (the bim-

Simulation von dreidimensionalen Gesteinsvorkommen zur Charakterisierung der Aufschlussstichprobenverzerrung in Block-In-Matrix Gesteinen (Bimrocks)

Die geotechnische und geohydrologische Charakterisierung von Block-in-Matrix Gesteinen (sogenannte Bimrocks) wie tektonische Melange, Störungsfurchen, Geschiebemergel und Erdrutschgeröll ist mit einigen Schwierigkeiten verbunden. Eine genaue und zuverlässige Charakterisierung ist jedoch extrem wichtig, da bekannterweise Blöcke oder die Größenverteilung der Gesteinsblöcke die Materialeigenschaften wie Durchlässigkeit, Scherfestigkeit und die Wahl des Bauverfahrens entscheidend beeinflussen. Geotechnische und hydrogeologische Methoden zur Baugrunduntersuchung wie Bohrungen und Aufschlusskartierung ergeben jedoch widersprüchliche Ergebnisse, da von ein- und zweidimensionalen Stichproben auf dreidimensionale Vorkommen geschlossen wird. Monte Carlo Computer Simulationen können zur Untersuchung der Verzerrungswerte verwendet werden, die bei der Ableitung der dreidimensionalen Gesteinsblockverteilung aus zweidimensionalen Darstellungen wie Aufschlusskarten oder Fotoaufnahmen entstehen. Die Simulation von zweidimensionalen Aufschlussdarstellungen von dreidimensionalen Gesteinen zeigt, dass Aufschlusskartierungen die Durchschnittsgesteinsgröße und das Gesamtvolumen um mehr als 10 % über- oder unterschätzen können, obwohl gleichförmige Gesteinsblöcke tendenziell unterschätzt werden. Die durch zweidimensionale Stichproben einfließende Fehlergrößenordnung bewegt sich im Bereich von ± 50 % für Durchschnittsgesteinsblöcke und ± 80 % für das Gesamtvolumen. Ein gründlich geplantes statis-

tisches Probenentnahmeprogramm von Gesteinsgröße und Ausrichtung in Verbindung mit numerischer Simulation birgt demnach die größte Chance auf verwendbare Information bezüglich der Gesteinsverteilungsstatistik, die wesentlichen Einfluss auf die Ingenieurplanung und Bauausführung haben kann.

Geotechnical and hydrogeological characterization of block-in-matrix rocks (bimrocks) such as melange, fault gouge, till, and landslide debris can be difficult, but accurate and reliable characterization is important because block or block size distributions are known to influence factors such as permeability, shear strength, and the choice of construction methods. Geotechnical and hydrogeological exploration methods such as drilling and outcrop mapping, however, produce biased results because they yield 1D or 2D samples of 3D populations. Monte Carlo computer simulations can be used to explore the amount of bias introduced when 3D block distribution information is inferred from 2D projections such as outcrop maps or photographs. Simulations of the 2D outcrop projections of 3D blocks show that outcrop mapping has the potential to overestimate or underestimate mean block sizes and total block volumes by tens of percent, although the tendency will be towards underestimation for blocks that are not highly elongated. The magnitudes of errors introduced by 2D outcrop sampling can be on the order of $\pm 50\%$ for mean block sizes and $\pm 80\%$ for total block volumes. Carefully designed statistical sampling of block sizes and orientations combined with numerical simulations, however, has the potential to yield valuable information about the statistics of block distributions that may have significant effects on the design and construction of engineered works.

Fig. 2 A) Oblique view showing the intersection of an ellipsoid (representing a bimrock block) intersecting a plane (representing an outcrop face). B) View perpendicular to the outcrop plane, illustrating the 2D ellipse formed by the intersection of the ellipsoid and the plane.

Bild 2 A) Schrägansicht eines Schnitts von Ellipsoid (Darstellung des Bimrock-Blocks) und Ebene (Darstellung der Aufschlussfläche). B) Lotrechte Ansicht der Aufschlussfläche zeigt die zweidimensionale Ellipse, die bei Verschneidung von Ellipsoid und Ebene entsteht.

rock matrix in this case), but information about bimrock block proportions can allow the use of more optimistic strength estimates (4). At the same time, however, the practitioner must consider the uncertainty associated with block proportion estimates in order not to overestimate the strength added by blocks (5) or risk serious underestimation of the volume of blocks that may be encountered during construction. An accurate prediction of the largest blocks to be encountered during tunneling or excavation may also be critical in the selection of appropriate methods and machinery, but the scale-independent fractal (or nearly fractal) distribution of bimrock blocks makes this a difficult proposition (1, 5, 6).

Blocks with permeability that is appreciably higher or lower than that of the surrounding matrix can also affect groundwater flow. Although he did not use the term “bimrock”, Haneberg (7) used a series of analytical and numerical

groundwater flow models to show how zones of anomalously high or low permeability could control the directions and magnitudes of seepage force vectors in potentially unstable slopes, in some cases creating localized zones of instability. The size, spacing, and permeability contrast of blocks should therefore be important considerations in the hydrogeologic characterization of bimrocks.

Most previous studies of bimrock sampling bias and block distribution characterization have been based on the application of stereological principles to measurements of blocks from borehole core and logs, outcrop maps of real bimrocks in the field, and scale-model bimrocks created in the laboratory (1, 6, 7, 8, 9). Medley (1) concluded that, although sampling can in some cases reliably replicate the mean or median block size, there is in general little equivalence between 1D chord lengths (e.g. from the intersection of blocks and borings or from outcrop scanlines) measured on maps and the true 3D block size distributions. As might be expected from consideration of the geometry of the problem, 1D sampling consistently underestimates the relative proportions of the largest blocks and overestimates the relative proportions of the smallest blocks.

In this paper, the 2D projection or expression of 3D blocks is referred to as the outcrop effect. One way to mathematically estimate the bias introduced by inferring bimrock block sizes from an outcrop face is to use an apparent radius, which is the radius of the circle formed by a sphere (representing a bimrock block) intersecting a plane (representing an outcrop face). The mean apparent radius of a group of spheres that have a true radius r and are randomly oriented relative to the outcrop plane can be found by solving the equation for a circle

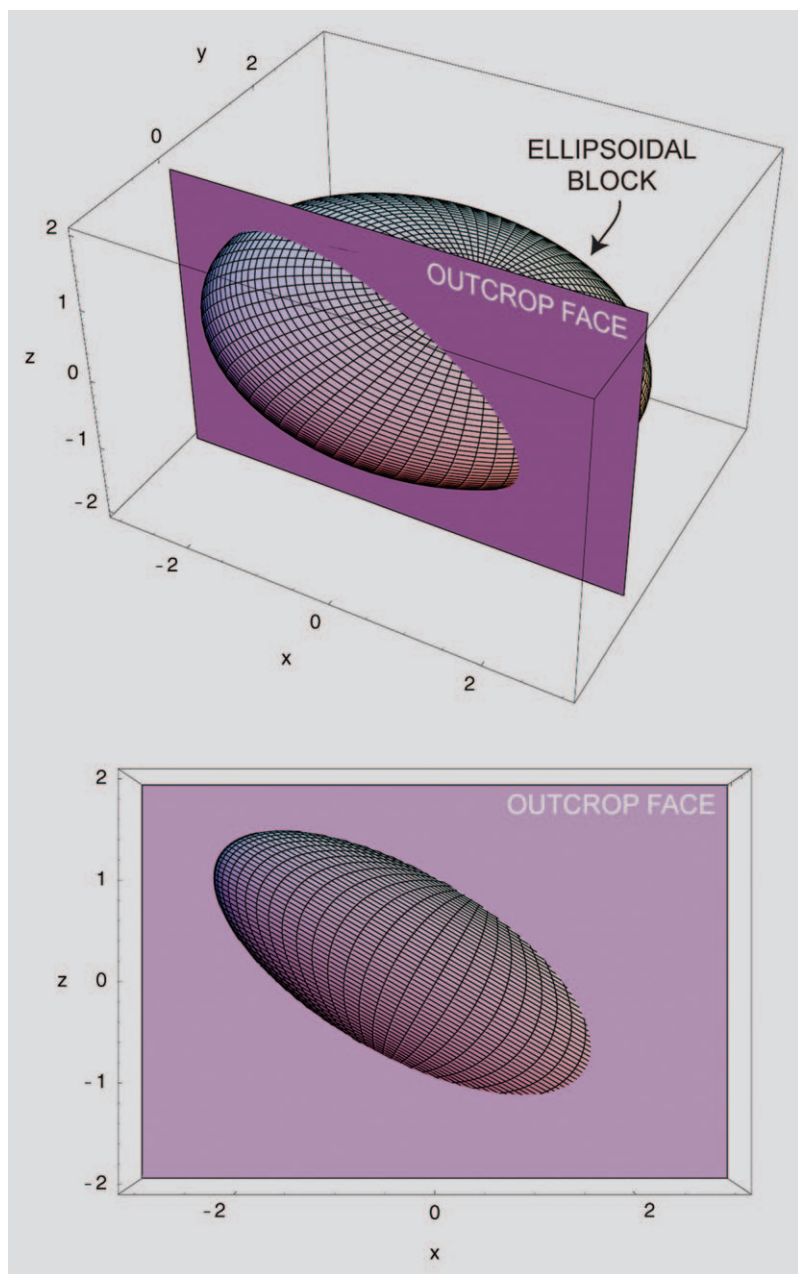
$$x^2 + y^2 = r^2 \dots\dots\dots [1]$$

for y and then evaluating the expression

$$\bar{r}_{1D} = \frac{1}{r} \int_0^r y \, dx = \frac{1}{r} \int_0^r \sqrt{r^2 - x^2} \, dx = \frac{r\pi}{4} \dots\dots\dots [2]$$

The mean apparent radius for randomly located spheres cut by a planar outcrop face is therefore approximately $3/4 r$. If the underlying block population can be approximated as a group of uniform spheres, then the calculation of the true block radius from a population of apparent block radii is trivial and the outcrop effect is consistent because apparent radii observed in outcrops will always be less than the true radii of the spheres.

Real bimrock blocks, however, are in general neither spherical nor uniformly sized and naïve inferences based on an assumption of uniformly sized spherical boulders can significantly over- or under-estimate effective radii and block size distributions of non-spherical blocks. Because of these complications, there exist no direct solu-





DER BESSERE WEG.

Plasser & Theurer entlastet die Straße. Das Verladensystem der MFS-Serie unterstützt die Materialbewältigung im Gleis- und Tunnelbau. Die Einheiten können in beliebiger Anzahl zusammengestellt werden: als Förderbandstraße, als Silo mit nahezu unbegrenzter Speicherkapazität oder als Kombination beider.

Plasser & Theurer

Export von Bahnbaumaschinen Gesellschaft m.b.H.

A-1010 Wien · Johannesgasse 3 · Tel. (+43) 1 515 72 - 0 · Telefax (+43) 1 513 18 01

Plasser & Theurer

tions to the inverse problem of reconstructing 3D block size distributions from 1D borehole or 2D outcrop measurements. If something is known about block shape and orientation, and perhaps the true block size distribution, then several indirect methods can be used to infer 3D distribution statistics from borehole or outcrop measurements (10, 11). These methods use numerical Monte Carlo simulations to generate populations of 3D blocks, from which apparent block size distributions are calculated and compared to the distributions of block sizes observed in outcrops or thin sections. There does not appear to exist, however, a simple but universal empirical conversion factor that will allow the practicing engineer or geologist to reliably infer 3D block size distributions from 1D or 2D samples of non-spherical blocks. Indeed: as shown below, a major conclusion of this paper is that the practitioner should be wary of using any such conversion factors without understanding the underlying assumptions.

Method

The results described in this paper were obtained using Monte Carlo simulations of ellipsoids (representing bimrock blocks or, as they are referred to in this paper, blocks) cut by planes (representing outcrop faces) as illustrated in Figure 2. For each simulation, 100 randomly oriented ellipsoids were generated. Then, the ellipse formed by the intersection of each ellipsoid with a planar outcrop face was determined, apparent equivalent radii were calculated in order to represent each block size with a single scalar, and summary statistics such as the mean apparent block size and the apparent block volume were calculated. In contrast to the apparent block size used in this paper, Medley (8) and Medley and Lindquist (12) used the maximum observed dimension to characterize the sizes of bimrock blocks. Haneberg (13) gives details of the derivations and Monte Carlo simulations that are summarized below, and an analogous exercise can be performed to evaluate the apparent block size distributions produced by the intersection of linear boreholes with ellipsoidal blocks (W.C. Haneberg, 2004, unpublished data).

The general expression for an ellipsoid with arbitrary orientation and semi-major axes a, b, and c is (14):

$$(X - U) \cdot R^T \cdot V \cdot R \cdot (X - U) = 1 \dots\dots\dots [3]$$

in which X = {x, y, z} is a vector containing the three Cartesian coordinate directions, U = {Δx, Δy, Δz} is a displacement vector describing the center of the ellipsoid relative to the coordinate system origin.

The shape matrix V is a diagonal matrix containing the lengths of the three semi-major axes of the ellipsoid

$$V = \begin{bmatrix} a^{-2} & 0 & 0 \\ 0 & b^{-2} & 0 \\ 0 & 0 & c^{-2} \end{bmatrix} \dots\dots\dots [4]$$

Equation [3] can be written for the special case of a sphere by letting a = b = c in equation [4].

The rotation matrix R contains information about the angular orientation of the ellipsoid relative to the coordinate system and, as illustrated below, is the product of three component rotation matrices that can be defined using several different conventions. This paper will use roll, pitch, and yaw angles that have physical meanings and will be familiar to readers who have sailed a boat or flown an airplane. Roll (ψ) is the amount of rotation of the ellipsoid about the x axis, pitch (φ) is that about the z axis, and yaw (θ) is that about the y axis. R can be written as the dot product of roll, pitch, and yaw matrices

$$R = R_{roll} \cdot R_{pitch} \cdot R_{yaw} \dots\dots\dots [5]$$

in which

$$R_{roll} = \begin{bmatrix} 1 & 0 & 0 \\ 0 & \cos \psi & \sin \psi \\ 0 & -\sin \psi & \cos \psi \end{bmatrix} \dots\dots\dots [6]$$

$$R_{pitch} = \begin{bmatrix} \cos \phi & \sin \phi & 0 \\ -\sin \phi & \cos \phi & 0 \\ 0 & 0 & 1 \end{bmatrix} \dots\dots\dots [7]$$

$$R_{yaw} = \begin{bmatrix} \cos \theta & 0 & \sin \theta \\ 0 & 1 & 0 \\ -\sin \theta & 0 & \cos \theta \end{bmatrix} \dots\dots\dots [8]$$

The outcrop effect can be simulated by setting either x, y, or z = 0 in equation [3], which changes the equation from one describing an ellipsoid to one describing an ellipse lying in the plane of the other two coordinate axes. In the examples that follow, the outcrop effect was accomplished by setting z = 0 to obtain the equation for an ellipse in the x-y plane representing an outcrop face. Then, the offset Δz was varied randomly to simulate the effect of blocks located different distances from the outcrop plane. The equation for an inclined ellipse that is produced by setting, for example, z = 0 has the form

$$C_1 x^2 + C_2 xy + C_3 y^2 = 1 \dots\dots\dots [9]$$

in which C₁, C₂, and C₃ are real coefficients. At this point, equation [9] can be plotted for each ellipse to produce a graphical representation of the apparent block size distribution arising as a consequence of the outcrop effect. Calculation of the size of each ellipse requires additional work to determine its semi-axes, from which its area and apparent block size can be calculated. The two semi-axes of the ellipse are given by

$$\begin{Bmatrix} \hat{a} \\ \hat{b} \end{Bmatrix} = \frac{1}{\sqrt{\lambda}} \dots\dots\dots [10]$$

in which λ is a vector containing the two eigenvalues of the matrix

$$\begin{bmatrix} C_1 & C_2/2 \\ C_2/2 & C_3 \end{bmatrix} \dots\dots\dots [11]$$

It is convenient to represent the volume of the blocks using a scalar that has the same units for both the original ellipsoids and the ellipses formed on the outcrop plane. This can be accomplished using an equivalent radius, which is the radius of a circle having the same area as the ellipse or the radius of a sphere having the same volume as the ellipsoid. The equivalent radius of an ellipse in the outcrop plane, which is also by definition an apparent radius, is

$$r_{2D} = \sqrt{\hat{a} \hat{b}} \dots\dots\dots [12]$$

whereas the equivalent radius of the original ellipsoid is given by

$$r_{3D} = \sqrt[3]{abc} \dots\dots\dots [13]$$

The equivalent radius of an ellipse formed by the intersection of an ellipsoid with a plane is an apparent equivalent radius because its value will depend on the orientation and position of the ellipsoid relative to the outcrop plane. The equivalent radius of the ellipsoid, however, is not apparent because it is calculated using the actual values of a, b, and c. Once equivalent radii have been calculated for all of the ellipsoids and ellipses in a

Table 1 Geometric variables for the four Monte Carlo simulations.

Table 1 Geometrische Variablen für die vier Monte Carlo Simulationen.

Case	Axial ratio a : b : c	Equivalent radius size distribution	Outcrop offset	Roll ψ	Pitch ϕ	Yaw θ
I	3 : 2 : 1	constant	$0 \leq \Delta z \leq 1$	0°	0°	0°
II	3 : 2 : 1	constant	$0 \leq \Delta z \leq 1$	$\pm 10^\circ$	$\pm 10^\circ$	$\pm 10^\circ$
III	3 : 2 : 1	constant	$0 \leq \Delta z \leq 1$	$\pm 45^\circ$	$\pm 45^\circ$	$\pm 45^\circ$
IV	3 : 2 : 1	Pareto	$0 \leq \Delta z \leq 1$	$\pm 45^\circ$	$\pm 45^\circ$	$\pm 45^\circ$

simulation, the mean block size, block sorting, and other standard size distribution measures can be calculated and compared to evaluate the degree of bias introduced by the outcrop effect.

To illustrate the calculation of equivalent radii, consider an ellipsoid with semi-axes $a = 5$, $b = 3$, and $c = 1$ that is rotated 20° about the z-axis and intersects the x-y plane at $z = 0$. The ellipse formed by the intersection of the ellipsoid and the outcrop plane is

$$1 = 0.0483 x^2 - 0.0457 xy + 0.103 y^2 \dots\dots\dots [14]$$

which has the coefficient matrix eigenvalues $\lambda = \{0.111, 0.040\}$ and, from equation [10], semi-axes $\hat{a} = 5$ and $\hat{b} = 3$. Note that in this case $\hat{a} = a$ and $\hat{b} = b$ because there was no rotation around the x or y axes. In general, this will not be true. The apparent equivalent radius in the plane of the outcrop is, using equation [12], $r_{2D} = (5 \cdot 3)^{0.5} = 3.87$, which is larger than the ellipsoid equivalent radius of $r_{3D} = (5 \cdot 3 \cdot 1)^{0.33} = 2.47$ obtained from

INGENIEURBÜRO **LAABMAYR** & PARTNER ZT GmbH

- PLANUNG, STATIK
- AUSSCHREIBUNG
- BAUÜBERWACHUNG
- TUNNELPRÜFUNG
- GUTACHTEN, BERATUNG



TUNNELBAU



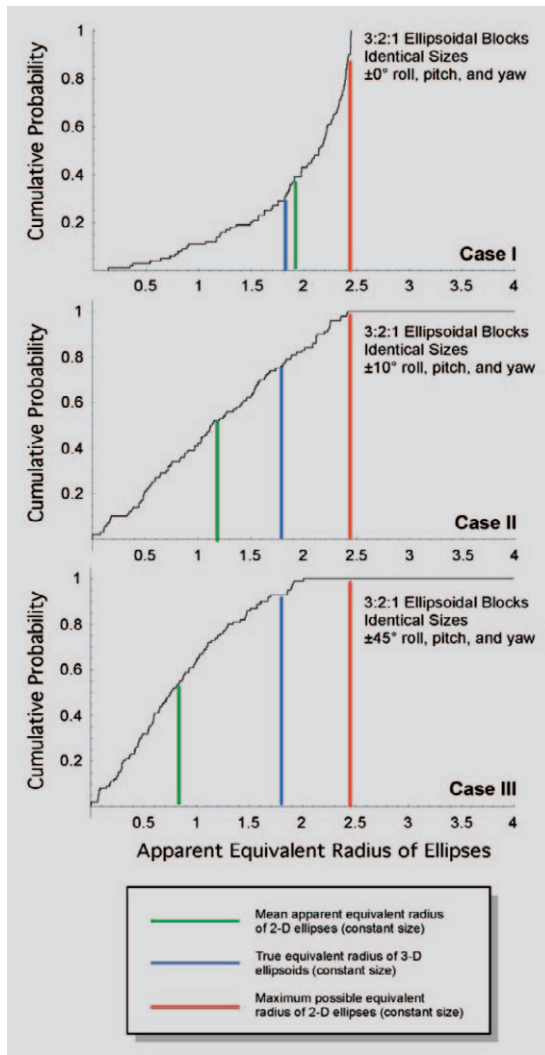
GRUNDBAU



A-5020 Salzburg, Preishartlweg 4, Tel. +43/662/430703-0, Fax -33
E-Mail: office@laabmayr.at Internet: www.laabmayr.at

Fig. 3 Apparent cumulative size distribution curves for 2D ellipses produced by the outcrop effect for case I, II, and III Monte Carlo simulations of 3D ellipsoids with uniform size located at random distances from the outcrop face. Red line: maximum possible apparent equivalent radius of an ellipse formed by the intersection of a 3 : 2 : 1 ellipsoid with the outcrop plane. Blue line: True equivalent radius of a 3 : 2 : 1 ellipsoid. Green line: Mean apparent equivalent radius of ellipses in each simulation. Variables as described in Table 1.

Bild 3 Summengrößenverteilungskurven für zweidimensionale Ellipsen, entstanden durch den Aufschlusseffekt für die Fälle I, II und III der Monte Carlo Simulationen von dreidimensionalen Ellipsoiden gleicher Größe mit unterschiedlicher Entfernung von der Aufschlussfläche. Rote Linie: größtmöglicher äquivalenter Radius, der bei der Verschneidung eines 3 : 2 : 1 Ellipsoids mit der Aufschlussfläche entsteht. Grüne Linie: Mittlerer äquivalenter Radius für Ellipsen in jeder der Simulationen. Variablen siehe Tabelle 1.



equation [13]. In this case, therefore, the outcrop effect would lead one to underestimate the largest dimension of the ellipsoid but overestimate the equivalent block radius of the ellipsoid.

Results

The results of four test cases illustrate the degree of bias that can be introduced by the outcrop effect (Table 1). Block orientation was allowed to vary but block size was held constant in the first three cases. In the fourth case, block sizes were specified using a fractal-like Pareto distribution of equivalent radii to simulate the apparent “well-graded” block size distribution that might arise from the fragmentation and shearing leading to the formation of a melange, fault rock, or perhaps landslide debris. Ellipsoids with semi-axis ratios of 3 : 2 : 1 were used in all of the simulations described in this paper, with the long and intermediate semi-axes of the ellipsoids originally parallel to the x-y outcrop plane. This corresponds to a bimrock with bullet- or torpedo-shaped ellipsoidal blocks. The outcrop offset for each ellipsoid was chosen at random from a uniform distribution with $0 \leq \Delta z \leq 1$. Haneberg (13) describes the results of a similar set of simulations using ellipsoids with 5 : 3 : 1 axial ratios.

The ellipsoids generated in Case I were offset from the outcrop face but not rotated ($\psi = \phi = \theta = 0$). As shown in Figure 3, the apparent cumulative block size distribution curve inferred from the ellipses in the outcrop plane overestimates the mean equivalent radius by approximately 5 % and overestimates the total block volume by 45 %, which is consistent with the concave-upward cumulative distribution curve that asymptotically approaches the maximum possible equivalent block size of $(3 \cdot 2)^{0.5} = 2.45$ length units (red lines in Figure 3). The blue lines in Figure 3 show the equivalent radius of the identically sized 3D ellipsoids, which is $(3 \cdot 2 \cdot 1)^{0.33} = 1.82$.

It is important to note that in the cumulative plots for cases I, II, and III there is no corresponding cumulative distribution for the 3D ellipsoids because the ellipsoids are all the same size; the apparent size distribution curve for the blocks is solely a result of the outcrop effect. The over-prediction of mean block size and total block volume is in part an artifact of the initial ellipsoid orientation relative to the outcrop plane. Had the intermediate and short axes been placed parallel to the outcrop, the ellipses in the outcrop plane likely would have underestimated the mean block size and volume.

If the roll, pitch, and yaw angles are all allowed to vary uniformly over a range of $\pm 10^\circ$ as in case II, however, the cumulative distribution curve approaches a straight line up to the theoretical limit of 2.45 (see Figure 3). The outcrop effect leads to an under-estimation of the mean equivalent radius by 35 % and under-estimation of the total block volume by 44 % in this simulation. As above, different results would have been obtained had the initial orientation of the ellipsoids or their axial ratios been different.

Rotation of the ellipsoids with roll, pitch, and yaw angles drawn from uniform distributions ranging over $\pm 45^\circ$ (case III) leads to a similar under-estimation of 54 % for the mean equivalent radius and 76 % for the total block volume. The three apparent block size distribution curves in Figure 3 show that the mean block size and total block volume errors increase as block orientation becomes more irregular even if the underlying 3D block size does not change.

Results from cases I, II, and III show the complexity that can arise due solely to the orientation and position of a population of identically sized ellipsoidal blocks relative to an outcrop face. The block size distribution of bimrocks such as melange and fault rocks, though, can be simulated using Pareto distributions that are closely related to fractal size distributions (15). Medley and Lindquist (12), in particular, discussed the engineering implications of fractal bimrock block size distributions.

The probability density function (PDF) of a Pareto distribution as implemented in the software used to perform the calculations in this paper is, using an approach described by Haneberg (13):

$$PDF(r_{3D}) = \alpha k^\alpha r_{3D}^{-(1+\alpha)} \quad r_{3D} \geq k \dots\dots\dots [15]$$

in which r_{3D} is the equivalent radius of an ellipsoid being simulated, $k > 0$ is the minimum possible radius, and α is a shape parameter that is equivalent to the fractal dimension of the distribution. This formulation is slightly different than the Pareto distribution given in some references, which assume a minimum value of zero and shift the abscissa by an increment k . The shape of the PDF curve and the geometric significance of α , however, are the same in both versions.

Published estimates of fractal dimensions for artificially and naturally produced rock fragments range from about 1.9 to 3.5, with a mean value in the range of 2.5 to 2.6 (15). Medley and Lindquist (12) estimated a fractal dimension of 2.3 for Franciscan Complex melanges in northern California. In this study, a value of $\alpha = 2.5$ was chosen as a typical fractal dimension for the case IV simulation. In order to generate a Pareto distribution with an average block size similar to those in cases I, II, and III, the mean equivalent radius of the Pareto-distributed blocks was set equal to the equivalent radii of the blocks used in the first three simulations $\bar{r}_{3D} = (3 \cdot 2 \cdot 1)^{0.33} = 1.82$. The analytical expression for the mean of the Pareto distribution is

$$\bar{r}_{3D} = \frac{k \alpha}{\alpha - 1} \dots\dots\dots [16]$$

Assuming a value of $\alpha = 2.5$, setting equation [16] equal to 1.82, and solving for k yields the value of $k = 1.12$, which was used in the case IV simulation.

The Case IV simulation results show the amount of complexity that is added to outcrop patterns when real block sizes are of random dimensions as well as the blocks having random orientation and position relative to the outcrop face (Figure 4). This situation is more typical of the disorder common in many bimrocks than are cases I, II, and III. In this simulation, the mean apparent equivalent radius was underestimated by 54 % and the total block volume was underestimated by 89 %. Comparison of the ellipsoid and ellipse cumulative distribution curves also shows that 21 % of the Pareto-distributed ellipsoids are likely to have equivalent radii greater than the largest value calculated from the 100 ellipses seen in the simulated outcrop. The probability that the largest ellipsoid in the underlying Pareto distribution has an equivalent radius more than twice as great as the largest block inferred from the ellipses in the outcrop plane is approximately 8 %. This result has significant economic and constructability implications for earthwork, excavation, or tunneling projects in which the size of the largest block expected to be encountered during excavation is inferred solely from uncorrected outcrop or borehole data.

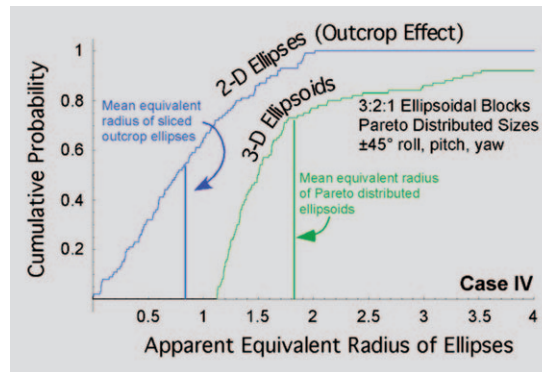


Fig. 4 Apparent cumulative size distribution curves for 2D ellipses produced by the outcrop effect for case IV Monte Carlo simulation of 3D ellipsoids with Pareto-distributed equivalent radii located at random distances from the outcrop face. Variables as described in Table 1.

Bild 4 Summengrößenverteilungskurven für zweidimensionale Ellipsen, entstanden durch den Aufschlussseffekt für Fall IV der Monte Carlo Simulationen von dreidimensionalen Ellipsoiden mit nach Pareto-verteilten äquivalenten Radien mit unterschiedlicher Entfernung von der Aufschlussfläche (Variablen siehe Tabelle 1).

described here, 1D borehole logs without supplementary 3D rock mass fabric data, has the potential to produce significant errors in estimated mean block sizes, maximum block sizes, and total block volumes. Results of the simple Monte Carlo simulations described in this paper suggest that inferred mean block sizes may be in error by as much as 50 % and block volumes by as much as 90 %. Perhaps most importantly for design and construction planning, outcrop or borehole sampling will almost inevitably underestimate the largest block likely to be encountered during a project. The sizes and volumes of spherical blocks will in all cases be under-estimated by outcrop sampling. The sizes and volumes of mildly elongated ellipsoidal blocks will tend to follow the

SCHALUNGSSYSTEME
VERBAUSYSTEME
GEOTECHNIK

Auftriebsicherung

von Wannen, Klärbecken im Grundwasser, weil die Zugfähigkeit die Betondecke nicht durchstoßen und Undichtigkeiten erzeugen.

Gründung von Schallschutzwänden

Schallschutzwand
Fahrbahn Standspur Bankkett

Unbekannte Hindernisse in aufgeschütteten Straßen oder Bahndämmen sind für Kleinverpresspfähle TITAN kein Problem.

Der Anker. Der Bodennagel. Die Injektionslanze. Der Pfahl.

Fundament-Verstärkung und Nachgründung

- ohne Aushub und Entsorgungsprobleme
- bei laufendem Betrieb
- ohne Wasserhaltung
- bei schwer zugänglichen Baustellen

FRIEDR. ISCHEBECK GMBH
POSTFACH 13 41 · D-58242 ENNEPETAU · TEL. (0 23 33) 83 05-0 · FAX (0 23 33) 83 05-55
E-MAIL: info@ischebeck.de · INTERNET: http://www.ischebeck.de

Conclusions

The inference of 3D bimrock block size distributions from 2D outcrop maps and, although not

same pattern of under-estimation, although exceptions are possible if the two longest axes of the ellipsoids are nearly parallel to the outcrop face. Perhaps most importantly, simple empirical measures relating factors such as apparent 1D or 2D block dimensions with actual 3D dimensions are likely to be of very limited, if any, utility to the practicing engineer or engineering geologist. These factors will depend very heavily on the block geometry and orientation, and will therefore differ from project to project.

The orientation of blocks relative to the outcrop face and block shape determine whether 2D sampling underestimates or overestimates 3D parameters. Therefore, an understanding of the 3D fabric of bimrocks should be considered an essential supplement to 2D outcrop or 1D borehole characterization projects. Knowledge of the local structural geology and regional tectonic setting of a project area, for example, can be used to estimate block orientation variability by applying spherical statistics to equal-area projections of rock fabric data. Sampling of alluvium derived from bimrocks may provide important constraints on block dimensions in cases where 3D exposures do not exist. In situations where the bimrock matrix is friable or otherwise unlithified, excavation and careful measurement of complete blocks should be considered an essential aspect of site characterization. Once this kind of information is obtained, practicing engineers and geologists can use indirect comparison methods such as those described by Sahagian and Proussevitch (10) to back-calculate true block size distributions.

References

1. Medley, E.W.: *Estimating block size distributions of melanges and similar block-in-matrix rocks (bimrocks)*. In: Hamamah, R. ; Bawden, W. ; Curran, J. ; Telesnicki, M. (eds.): Proceedings of the 5th North American Rock Mechanics Symposium (NARMS), pp. 599-606, 2002.
2. Lindquist, E.S.: *The mechanical properties of a physical model melange*. In: Olivera, R. ; Rodrigues, L.F. ; Coelho, A.G. ; Cunha, A.P. (eds.): Proceedings, 7th International Congress, International Association of Engineering Geology: Lisbon, Portugal, pp. 819-826, 1994.
3. Lindquist, E.S. ; Goodman, R.E.: *Strength and deformation properties of a physical model melange*. In: Nelson, P. ; Laubach, S.E. (eds.): Proceedings of the 1st North American Rock Mechanics Symposium, Austin, Texas, USA, pp. 843-850, 1994.

4. Goodman, R.E. ; Ahlgren, C.S.: *Evaluating safety of concrete gravity dam on weak rock: Scott Dam*. J. Geotechnical and Geoenvironmental Eng., Vol. 126 (2000), pp. 429-442.
5. Medley, E.: *Uncertainty in estimates of block volumetric proportions in melange bimrocks*. In: Marinos, P.G. ; Koukis, G.C. ; Tsiambaos, G.C. ; Stournaras, G.C. (eds.): Proc. International Congress, International Association of Engineering Geologists, Engineering Geology and the Environment, Athens, Greece, 1997.
6. Medley, E. ; Goodman, R.E.: *Estimating the block volumetric proportions of melanges and similar block-in-matrix rocks (bimrocks)*. In: Nelson, P.P. ; Laubach, S.E. (eds.): Proceedings of the 1st North American Rock Mechanics Symposium, Austin, Texas, USA, pp. 851-858, 1994.
7. Haneberg, W.C.: *Groundwater flow and the stability of heterogeneous infinite slopes underlain by impervious substrata*. In: Haneberg, W.C. ; Anderson, S.A., (eds.): Clay and Shale Slope Instability. Geological Society of America Reviews in Engineering Geology 10, pp. 63-78, 1995.
8. Medley, E.W.: *Engineering characterization of melanges and similar block-in-matrix rocks (bimrocks)*. Ph.D. dissertation, Department of Civil Engineering, University of California at Berkeley, 1994.
9. Medley, E.W.: *Using stereological methods to estimate the volumetric proportions of blocks in melanges and similar block-in-matrix rocks (bimrocks)*. In: Olivera, R. ; Rodrigues, L.F. ; Coelho, A.G. ; Cunha, A.P. (eds.): Proceedings 7th International Congress, International Association of Engineering Geology: Lisbon, Portugal, pp. 1031-1040, 1994.
10. Sahagian, D.L. ; Proussevitch, A.A.: *3D particle size distributions from 2D observations; stereology for natural applications*. Journal of Volcanology and Geothermal Research, Vol. 84 (1998), pp. 173-196.
11. Higgins, M.D.: *Measurement of crystal size distributions*. American Mineralogist, Vol. 85 (2000), pp. 1105-1116.
12. Medley, E. ; Lindquist, E.S.: *The engineering significance of the scale-independence of some Franciscan melanges in California, USA*. In: Daemen, J.J.K. ; Schultz, R.A. (eds.): Rock Mechanics, Proceedings of the 35th U.S. Symposium, Reno, Nevada, pp. 907-914, 1995.
13. Haneberg, W.C.: *Computational Geosciences with Mathematica*. Berlin, Heidelberg, New York: Springer-Verlag, 2004.
14. Herbison-Evans, D.: *Animated Cartoons by Computer Using Ellipsoids*. University of Sydney, Basser Department of Computer Science, Technical Report 94, (online version) <http://linus.it.uts.edu.au/~don/pubs/cartoon.html> (2002).
15. Turcotte, D.L.: *Fractals and Chaos in Geology and Geophysics*. 2nd ed. Cambridge: University Press, 1997.

Acknowledgements

My interest in bimrock sampling and simulation was motivated by many conversations with Ed Medley, whose contributions and references are greatly appreciated. Wolfram Research, Inc. donated a copy of the Mathematica software used in this research. Thanks also to Isabelle Pawlik, PE, of Jacobs Associates, San Francisco for the German translations.

Author

William C. Haneberg, Haneberg Geoscience, 10208 39th Avenue SW, Seattle WA 98146 USA, E-Mail bill@haneberg.com



Ing. Mag. Gernot SCHEFZIK

Ingenieurkonsulent
für Technische Geologie

Allgemein beeideter und
gerichtlich zertifizierter Sachverständiger



A-9500 Villach, Wilhelm Backhausstraße 16; Tel.: +43(0)4242/54693-1, Fax: +43(0)4242/54693-4, Mobil: +43(0)664/2116950
e-mail: zt-schefzik@utanet.at

Ingenieurgeologie – Hydrogeologie – Planung und Überwachung von
Untertagebauwerken – Begleitende Kontrolle und Projektmanagement
Tunnel- und Stollenprüfungen